# ChemComm

Chemical Communications

## Accepted Manuscript

Volume 54
Number 1
4 January 2018
Pages 1-112

# ChemComm

Chemical Communications

rsc.li/chemcomm

ISSN 1359-7345

**COMMUNICATION**
S. J. Connon, M. O. Senge et al.
Conformational control of nonplanar free base porphyrins:
towards bifunctional catalysts of tunable basicity

**ROYAL SOCIETY OF CHEMISTRY**

**ROYAL SOCIETY OF CHEMISTRY**

rsc.li/chemcomm

# COMMUNICATION

**ChemComm Accepted Manuscript**

## Layered assembly of cationic and anionic supramolecular polymers

Jovana Jevric, Simon M. Langenegger, and Robert Häner[*]

**The chemical synthesis and the supramolecular assembly of an aromatic oligoamine are described. The self-assembly of the cationic oligomers in aqueous solution leads to the formation of vesicular objects. The assembly process of the oligomers is monitored by absorption and fluorescence spectroscopy and the formed vesicles are characterized by atomic force and transmission electron microscopy. The electrostatic complementarity of anionic supramolecular polymers sheets and the cationic vesicles is used for a layered assembly process.**

The field of supramolecular polymers is rapidly expanding.[1–4] The properties of supramolecular polymers, such as self-healing, remouldability and easy recyclability, may lead to future-oriented types of application.[5–8] In addition to the commonly used organic solvents, also aqueous conditions can be used for the self-assembly of supramolecular polymers.[9] In particular, the employment of water as a medium opens the possibility of using highly polar and even ionic compounds as building blocks for the assembly of supramolecular systems. Supramolecular polymers assembled in aqueous medium find applications in biomedical engineering[2,9–16], sensing[17], organic electronics,[18] light harvesting[19–23] and solar energy conversion.[9,24] For the assembly of supramolecular structures with special spectroscopic and light-harvesting properties, π-conjugated and aromatic molecules are of particular interest.[2,9] We have previously observed light-harvesting properties in various types of supramolecular assemblies of oligophosphates based on phenanthrenes and tetraphenylethylene in aqueous medium.[19–21,25] Further, pyrene trimers showed interesting spectroscopic properties due to their self-assembly into nanosheets.[26] These polyaromatic oligomers were joined by phosphodiester linkages and, thus, were of anionic nature.[19,26–29] Besides these examples of polyphosphoester oligomers,[29–32] amine-linked polyaromatic oligomers have not been studied in this context. Under physiological conditions, an amine-based connecting unit will lead to the formation of cationic oligomers with, presumably, different chemical properties. In addition, access to cationic oligomers would bring the further option of forming and studying composites with anionic phosphodiester-linked oligomers. The method of electrostatic layering was first applied in the 60's by Iler[33] and Kirkland,[34] who both made use of microparticles. Around 30 years later, Decher revived the method by the application on a wide range of polyelectrolytes.[35,36] The method has since been used for the preparation of ultrathin-layers and is of high interest for the production of optics and sensors.[37–43] Herein, we present the synthesis, the self-assembly and the spectroscopic properties of a 3,6-dialkynyl-substituted, amine-linked phenanthrene-trimer (**N-Phe₃**, Scheme 1). Additionally, the cationic oligomer was used for the formation of nanometer-scaled aggregates in an electrostatic layered assembly[36,38] in combination with an anionic supramolecular polymer.

The synthesis of the target compound **N-Phe₃**, the amino-linked trimer of 3,6-dipentynyl substituted phenanthrene, is depicted in Scheme 1. First, 4,4'-dibromo-trans-stilbene (**1**) was converted into 3,6-dibromophenanthrene (**2**) via oxidative photochemical cyclization in analogy to the literature.[44] A Sonogashira cross-coupling reaction afforded a mixture of compounds **3** and **4**, which were separated by flash column chromatography. Treatment of compound **3** with hydrazine afforded the amine **5**. Separately, the diol **4** was converted into the bis-aldehyde **6** by a Dess-Martin oxidation. A reductive amination reaction with compounds **5** and **6** finally yielded the oligomer **N-Phe₃**, which was purified by preparative TLC (ESI).

*Department of Chemistry, Biochemistry and Pharmacy, University of Bern, Freiestrasse 3, CH-3012 Bern, Switzerland. E-mail: robert.haener@dcb.unibe.ch; http://haener.dcb.unibe.ch*

**COMMUNICATION**
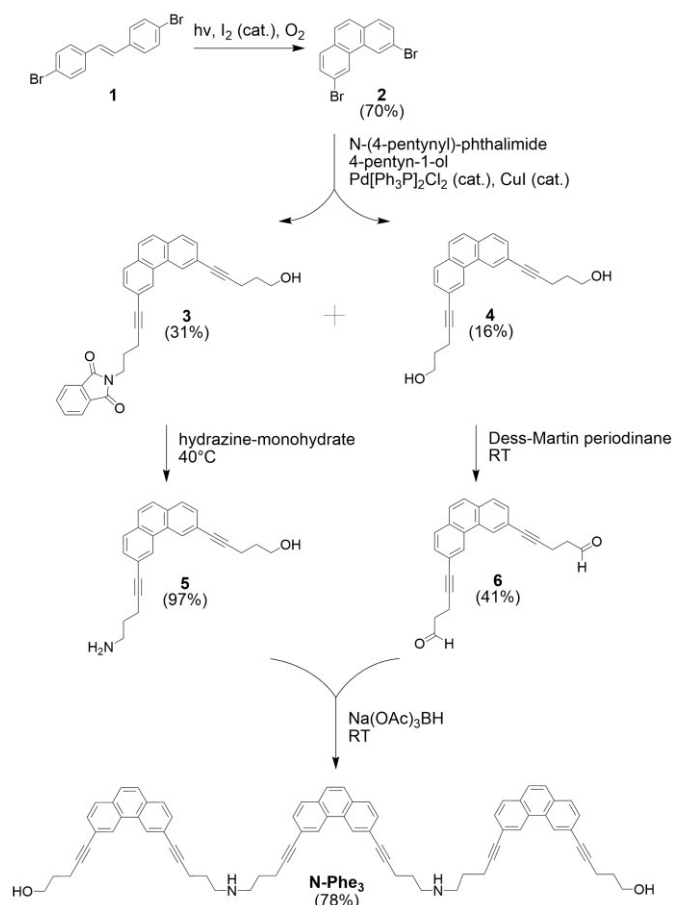
**Scheme 1** Synthesis of the 3,6-disubstituted phenanthrene trimer with amine-bridges (**N-Phe₃**).

Figure 1 shows the absorption spectra of **N-Phe₃** under different conditions. In ethanol, **N-Phe₃** exhibits a spectrum with three major absorption maxima at 253 nm, 314 nm, and 329 nm (black). **N-Phe₃** is soluble in ethanol and the spectrum closely resembles the one of phenanthrene monomer.[19] In aqueous medium (sample preparation see ESI), a distinct shift in the long-wavelength absorption bands is observed when the spectra are taken at elevated (75 °C) or at low (15 °C) temperature, which suggests a
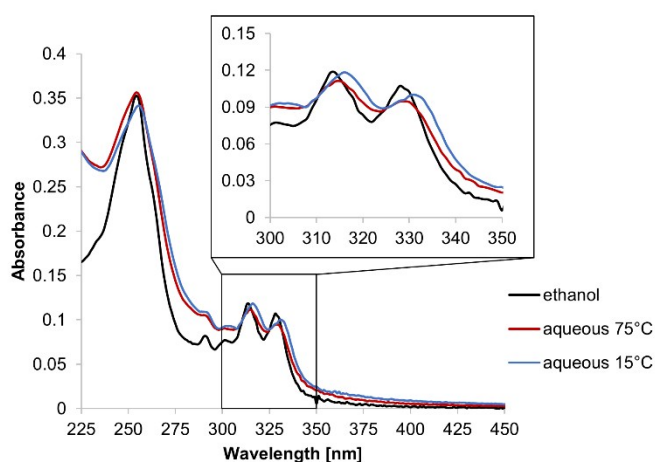


**Figure 1** UV-vis spectra of **N-Phe₃** (1 µM) in ethanol (black) and in an aqueous medium (10 mM sodium acetate buffer pH 4.7, containing 10 vol% ethanol) at 75 °C (red) and 15 °C (blue).
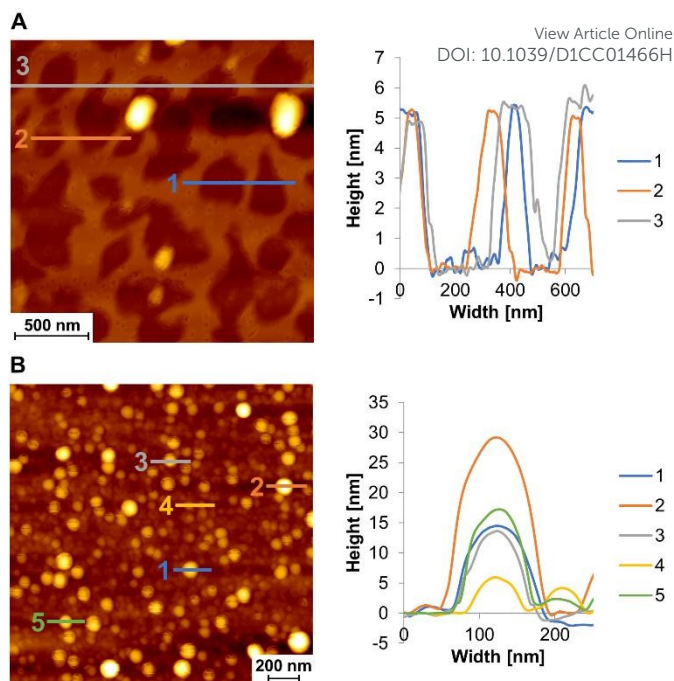
**Figure 2** AFM images of self-assembled structures obtained from amine-oligomer **N-Phe₃** at 1 µM and 10 µM sample concentrations (images A and B, respectively). Conditions: 10 mM sodium acetate buffer (pH 4.7), 10 vol% ethanol.

self-assembly process of **N-Phe₃** in this temperature range. At 75 °C the maxima (315 and 329 nm) correlate well with the ones observed in ethanol, which indicates that the oligomer is not assembled. Lowering the temperature leads to the self-assembly of **N-Phe₃** and a bathochromic shift of approximately 3 nm (317 and 332 nm). This redshift is explained by a structural change during the self-assembly of trimers upon lowering the temperature. Stepwise temperature-dependent recording of the spectrum reveals that the red-shift, and thus the self-assembly process, occurs in the range between 35 °C to 45 °C (ESI).

The morphology of the objects formed by self-assembly of **N-Phe₃** was investigated by atomic force microscopy (AFM) on mica. As shown in Figure 2, the sample concentration has a strong effect on the course of the self-assembly. At a 1 µM concentration (Figure 2A), the formation of a layer was observed in which coherent areas are separated by intervening holes. The average height of 5-6 nm suggests that the covered areas correspond to a bilayer of trimers (Figure 3). After the increase of the **N-Phe₃** concentration to 10 µM, vesicles were observed (Figure 2B). This type of concentration dependence in AFM imaging was already noticed in previous work.[27] Apparently, vesicles formed in the solution first, form the mentioned bilayer after deposition on mica. At higher concentrations (10 µM), vesicles are further adsorbed on this preformed bilayer. The vesicles exhibit a height of 6-30 nm and a width of 50-100 nm (Figure 2B).

The aqueous environment and hydrophobic effects favor stacking interactions between the phenanthrenes in the bilayer. The linkers with the amine and hydroxyl groups are pointing to the inner and outer side of the vesicles, as illustrated in Figure 3. Under the experimental conditions (pH 4.7), the amino groups are protonated, hence the vesicles are positively charged (zeta-potential = +3.72 ± 0.14 mV).

**Journal Name**
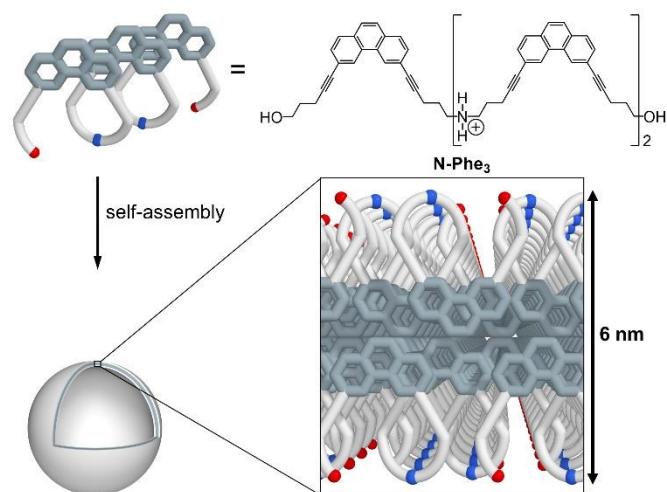
**Figure 3** Graphical illustration of vesicle formation by **N-Phe₃**. Blue dots indicate amines, red dots hydroxyl groups. A bilayer of trimers has a calculated height of ~6 nm.

The structural observations made by AFM were supported by transmission electron microscopy (TEM) experiments, which confirmed the formation of vesicles by **N-Phe₃** (Figure 4). The vesicles exhibited a diameter range from 50 nm up to 100 nm, which closely correlates with observations made by AFM. Dynamic light scattering (DLS) measurements revealed an average particle size of around 150 nm at 20 °C (ESI).

The above described positively charged vesicular assemblies of amine-linked oligomer **N-Phe₃** were next used for electrostatic layered assembly experiments in combination with negatively charged supramolecular nanosheets. The latter were assembled from a phosphodiester-linked, 1,6-disubstituted pyrene trimer (**Py₃**, see ESI), as described previously.[26] The 2-dimensional shape of this supramolecular polymer was considered as an ideal starting platform for the subsequent layering process. For the electrostatic assembly, the supramolecular objects, cationic vesicles and anionic nanosheets, were prepared independently with the trimers **Py₃** and **N-Phe₃** (Figure 5A and ESI). Figure 5B illustrates the formation of an electrostatic assembly, starting from an anionic **Py₃**-nanosheet on APTES-modified mica (positively charged). This first **Py₃**-layer is followed by a layer of positively charged **N-Phe₃** which adsorbs on the **Py₃**-sheet.[45] Unlike the vesicular shape on the unmodified mica (Figure 2A), **N-Phe₃** appears as a layer of discs on the negatively charged **Py₃**-sheets (Figure 5B). We attribute this difference to the change of the surface charge.
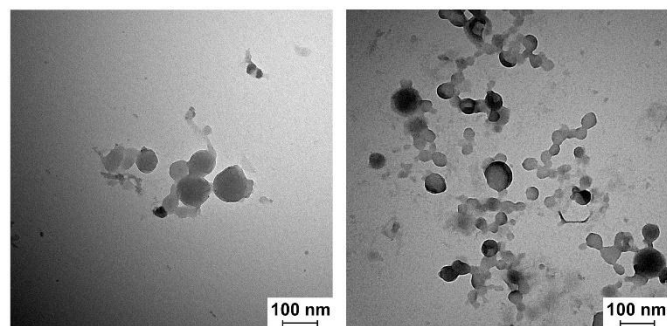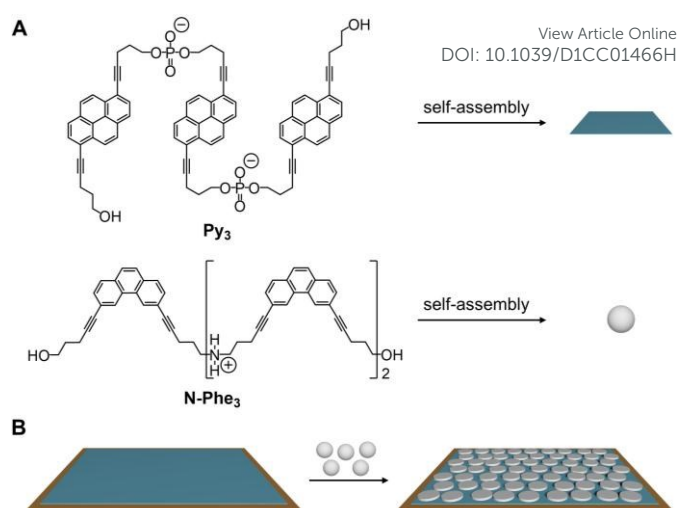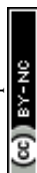


**Figure 5** Graphical illustration of the electrostatic layered assembly preparation. A) **Py₃** self-assembles into negatively charged sheets (blue) and **N-Phe₃** into positively charged vesicles (grey). B) First the **Py₃**-sheet (blue) is adsorbed on the substrate (APTES-modified mica, brown), followed by the adsorption of **N-Phe₃**-vesicles (grey).
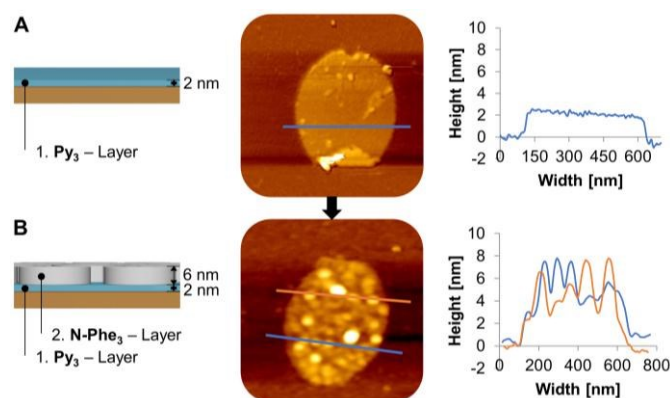


**Figure 6** Electrostatic assembly starting with **Py₃** sheets and leading to a two-layered structure. Left: graphical illustration of layering; middle and right: AFM images and height profiles. Conditions: 1st layer 2 μM **Py₃**, 10 mM sodium phosphate (pH 7.1), 10 mM NaCl and 10 vol% ethanol; 2nd layer 10 μM **N-Phe₃**, 10 mM sodium acetate buffer (pH 4.7) and 10 vol% ethanol.

Figure 6 shows the AFM images of the layering process according to Figure 5B. The first layer consists of **Py₃**-sheets adsorbed on APTES modified mica[46] with a height of 2 nm (Figure 6A). In a next step the second layer, **N-Phe₃**-vesicles, is added, which results in a total height of 8 nm for the two layers (Figure 6B). The height of 8 nm consists of the **Py₃**-sheets (2 nm) and the **N-Phe₃**-vesicles, which are adsorbed as bilayer discs (6 nm).

In conclusion, we have described the synthesis and self-assembly properties of a water-soluble amine-bridged phenanthrene oligomer (**N-Phe₃**). The oligomer self-assembles into vesicles in aqueous medium as shown by atomic force and electron microscopy. In addition, the cationic vesicles give rise to novel types of electrostatically controlled layered assemblies in combination with anionic supramolecular two-dimensional polymers, which was confirmed by AFM. Electrostatically controlled deposition of supramolecular polymers enables the buildup of layered nanomaterials. With well-defined dimensions and properties of the individual tiers, such nanocomposites are of interest for the field of



**Figure 4** TEM images of vesicles assembled from **N-Phe₃** (left: 3 μM; right: 5 μM). Conditions as in Figure 2.

molecular electronics, as sensors or as components of light-harvesting materials.

## Conflicts of interest

There are no conflicts to declare.

## Notes and references

1    T. Aida, E. W. Meijer and S. I. Stupp, *Science*, 2012, **335**, 813–817.
2    L. Yang, X. Tan, Z. Wang and X. Zhang, *Chem. Rev.*, 2015, **115**, 7196–7239.
3    J. F. Lutz, J. M. Lehn, E. W. Meijer and K. Matyjaszewski, *Nat. Rev. Mater.*, 2016, **1**, 1–14.
4    S. P. W. Wijnands, E. W. Meijer and M. Merkx, *Bioconjug. Chem.*, 2019, **30**, 1905–1914.
5    T. Aida and E. W. Meijer, *Isr. J. Chem.*, 2020, **60**, 33–47.
6    Y. Yang and M. W. Urban, *Chem. Soc. Rev.*, 2013, **42**, 7446–7467.
7    B. Rybtchinski, *ACS Nano*, 2011, **5**, 6791–6818.
8    E. A. Appel, J. del Barrio, X. J. Loh and O. A. Scherman, *Chem. Soc. Rev.*, 2012, **41**, 6195–6214.
9    E. Krieg, M. M. C. Bastings, P. Besenius and B. Rybtchinski, *Chem. Rev.*, 2016, **116**, 2414–2477.
10   S. I. Stupp, *Nano Lett.*, 2010, **10**, 4783–4786.
11   R. Dong, Y. Zhou, X. Huang, X. Zhu, Y. Lu and J. Shen, *Adv. Mater.*, 2015, **27**, 498–526.
12   C. Gong, S. Sun, Y. Zhang, L. Sun, Z. Su, A. Wu and G. Wei, *Nanoscale*, 2019, **11**, 4147–4182.
13   K. Petkau-Milroy and L. Brunsveld, *Org. Biomol. Chem.*, 2013, **11**, 219–232.
14   E. Stulz, *Acc. Chem. Res.*, 2017, **50**, 823–831.
15   S. K. Albert, M. Golla, N. Krishnan, D. Perumal and R. Varghese, *Acc. Chem. Res.*, 2020, **53**, 2668–2679.
16   D. Bousmail, P. Chidchob and H. F. Sleiman, *J. Am. Chem. Soc.*, 2018, **140**, 9518–9530.
17   C. A. E. Hauser, S. Maurer-Stroh and I. C. Martins, *Chem. Soc. Rev.*, 2014, **43**, 5326–5345.
18   T. M. Figueira-Duarte and K. Müllen, *Chem. Rev.*, 2011, **111**, 7260–7314.
19   C. B. Winiger, S. Li, G. R. Kumar, S. M. Langenegger and R. Häner, *Angew. Chemie - Int. Ed.*, 2014, **53**, 13609–13613.
20   S. Rothenbühler, I. Iacovache, S. M. Langenegger, B. Zuber and R. Häner, *Nanoscale*, 2020, **12**, 21118–21123.
21   J. Jevric, S. M. Langenegger and R. Häner, *Eur. J. Org. Chem.*, 2020, **2020**, 4677–4680.
22   J. G. Woller, J. K. Hannestad and B. Albinsson, *J. Am. Chem. Soc.*, 2013, **135**, 2759–2768.
23   H. Bui, S. A. Díaz, J. Fontana, M. Chiriboga, R. Veneziano and I. L. Medintz, *Adv. Opt. Mater.*, 2019, **7**, 1900562.
24   Y. Zeng, J. Chen, T. Yu, G. Yang and Y. Li, *ACS Energy Lett.*, 2017, **2**, 357–363.
25   M. Kownacki, S. M. Langenegger, S. X. Liu and R. Häner, *Angew. Chemie - Int. Ed.*, 2019, **58**, 751–755.
26   M. Vybornyi, A. V. Rudnev, S. M. Langenegger, T. Wandlowski, G. Calzaferri and R. Häner, *Angew. Chemie - Int. Ed.*, 2013, **52**, 11488–11493.
27   C. D. Bösch, J. Jevric, N. Bürki, M. Probst, S. M. Langenegger and R. Häner, *Bioconjug. Chem.*, 2018, **29**, 1505–1509.
28   R. Szweda, M. Tschopp, O. Felix, G. Decher and J. F. Lutz, *Angew. Chemie - Int. Ed.*, 2018, **57**, 15817–15821.
29   N. Appukutti and C. J. Serpell, *Polym. Chem.*, 2018, **9**, 2210–2226.
30   M. Vybornyi, Y. Vyborna and R. Häner, *Chem. Soc. Rev.*, 2019, **48**, 4347–4360.
31   R. Häner, F. Garo, D. Wenger and V. L. Malinovskii, *J. Am. Chem. Soc.*, 2010, **132**, 7466–7471.
32   N. F. König, S. Telitel, S. Poyer, L. Charles and J. F. Lutz, *Macromol. Rapid Commun.*, 2017, **38**, 1–5.
33   R. K. Iler, *J. Colloid Interface Sci.*, 1966, **21**, 569–594.
34   J. J. Kirkland, *Anal. Chem.*, 1965, **37**, 1458–1461.
35   G. Decher and J. Hong, *Makromol. Chem., Macromol. Symp.*, 1991, **46**, 321–327.
36   G. Decher and J. D. Hong, *Ber. Bunsenges. Phys. Chem.*, 1991, **95**, 1430–1434.
37   J. J. Richardson, J. Cui, M. Björnmalm, J. A. Braunger, H. Ejima and F. Caruso, *Chem. Rev.*, 2016, **116**, 14828–14867.
38   Y. Wang and X. Zhan, *Adv. Energy Mater.*, 2016, **6**, 1–18.
39   U. Akiba, D. Minaki and J. I. Anzai, *Polymers*, 2017, **9**, 553.
40   D. Rawtani and Y. K. Agrawal, *Nanobiomedicine*, 2014, **1**, 8.
41   J. J. Richardson, M. Björnmalm and F. Caruso, *Science*, 2015, **348**, aaa2491.
42   R. M. Iost and F. N. Crespilho, *Biosens. Bioelectron.*, 2012, **31**, 1–10.
43   K. Ariga, M. Nishikawa, T. Mori, J. Takeya, L. K. Shrestha and J. P. Hill, *Sci. Technol. Adv. Mater.*, 2019, **20**, 51–95.
44   H. R. Talele, A. R. Chaudhary, P. R. Patel and A. V. Bedekar, *Arkivoc*, 2011, **2011**, 15–37.
45   E. I. Goksu, J. M. Vanegas, C. D. Blanchette, W. Lin and M. L. Longo, *BBA - Biomembr.*, 2009, **1788**, 254–266.
46   L. S. Shlyakhtenko, A. A. Gall and Y. L. Lyubchenko, *Methods Mol Biol.*, 2013, **931**, 1–20.

**ChemComm Accepted Manuscript**